ELSEVIER

Polymer 40 (1999) 4307–4313

polymer

# Strong interaction at interface of carbon fiber reinforced aromatic semicrystalline thermoplastics

Tie Qi Li[a,b], Ming Qiu Zhang[a,*], Han Min Zeng[c]

[a]Materials Science Institute, Zhongshan University, Guangzhou 510275, People's Republic of China
[b]Department of Materials Science and Engineering, Guangdong University of Technology, Guangzhou 510090, People's Republic of China
[c]Laboratory of Polymeric Composite and Functional Materials, The State Educational Commission of China, Zhongshan University, Guangzhou 510275, People's Republic of China

Received 17 June 1998; received in revised form 18 August 1998; accepted 9 September 1998

---

**Abstract**

The interfacial structure of carbon fiber/polyetheretherketone (CF/PEEK) composites has been studied with Raman and X-ray photoelectron spectroscopy. Analysis of the fibers isolated from the composites proved that the polymer segments tended to form strong interactions with the fiber on the surface. Study of the fiber with a thin layer of PEEK coating further revealed that melting of the polymer plays an important role in forming the strong interfacial interaction. In connection with the above experimental results obtained from model systems with extremely low polymer content, the physical nature of the interfacial interaction is known through Raman spectroscopic observation of actual composites. Electronic matching between graphite crystallites of carbon fiber and the segments in special conformation is proved to be among the most important features of the intercalation-type interaction. © 1999 Elsevier Science Ltd. All rights reserved.

*Keywords:* Semicrystalline thermoplastics; Interfacial interaction; Composites

---

## 1. Introduction

It is known that stress transfer efficiency in a polymer composite depends on the structure between reinforcement and the matrix [1–5]. Characterization of the interfacial structure, however, is generally difficult [6,7], because materials in the interfacial region, referred to as an interphase or interlayer, occupy a small volume percentage of the composite.

In the case of thermosetting composites, the problem was circumvented through experimental studies on model systems, usually consisting of a substrate similar to the composite reinforcement and pre-polymers of interest [8–12]. By means of thermal and viscoelastic studies of practical composites [13], it was finally revealed that the interphase is the transitional region between organic components and an inorganic phase [12–15]. Strong interfacial interactions on the short-range, namely chemical bonds [9], and weak interfacial interactions such as a hydrogen bond [11], have been proved to be among the principal factors that contribute to stress transfer.

With respect to thermoplastic composites, interfacial structure is less understood. While dispersive bonds can also be expected to be present at the interface, strong short-range interactions other than that through end groups of polymers has not been known to the authors' knowledge. This makes it difficult to understand the enhancement of interfacial adhesion with a rise in processing temperature or in melt residual time found in aromatic polymer composites such as carbon fiber reinforced polycarbonate (PC) [16,17] and polyetheretherketone (PEEK) [18–22].

To solve the dilemma, a high strength PAN-based carbon fiber and the polymer PEEK were chosen in the present work. Fibers isolated from the composites were studied to see whether there is a strong interaction between the two components. The structure of the fibers coated with a thin layer of PEEK was characterized to probe into the effects of polymer melting. Based on the results from these model systems, Raman spectra of practical high-volume content composites were analyzed with the objective to reveal the nature of the short-range fiber–polymer interaction.

## 2. Experimental

The polymer, Victrex PEEK, with viscosity molecular

---

* Corresponding author: Tel.: + 86-20-84186300 ext. 2576; Fax: + 86-20-84186564.
*E-mail address:* ceszmq@zsulink.zsu.edu.cn (M.Q. Zhang)

PII: S0032-3861(98)00658-2

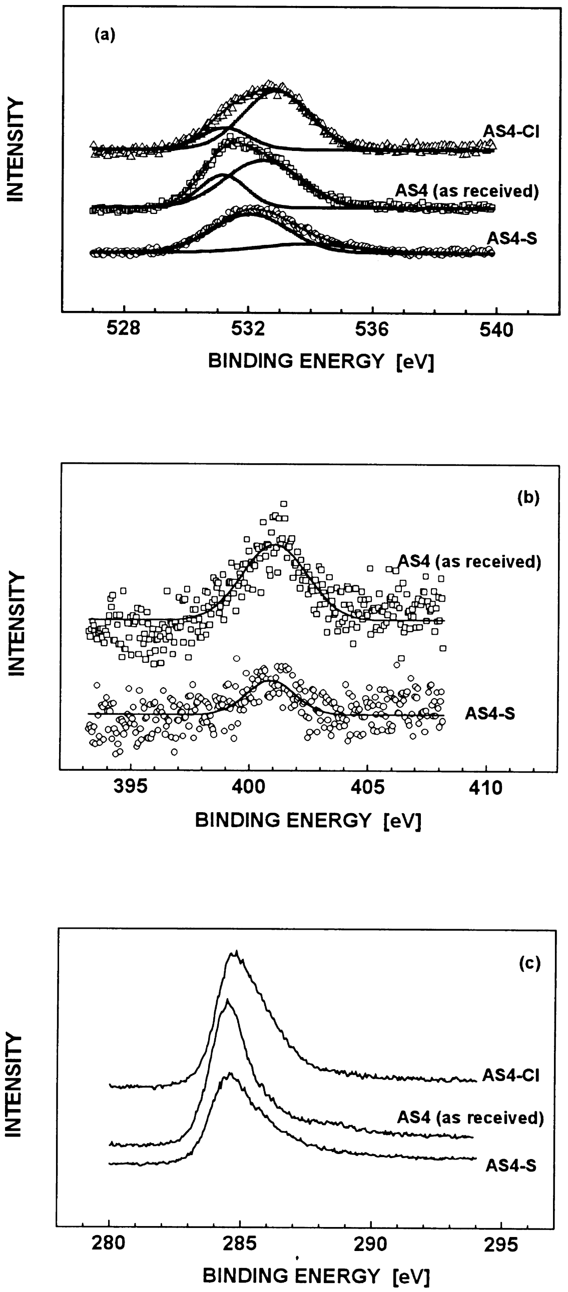

Fig. 1. XPS spectra of AS4 carbon fibers as-received and the extracted versions from APC-2 laminates: (a) O1s, (b) N1s, (c) C1s. Spectra were all normalized to avoid effects of fiber alignment.

weight of 29 300, and the 16-ply APC-2 laminates (consisting of AS4 carbon fiber and PEEK with fiber fraction of 60 vol.%) were produced by ICI. The PAN-based carbon fiber, AS4, is a size-free product of Hercules. The AS4/PEEK prepregs were prepared by the Aeromaterial Research Institute, Beijing, through the powder pre-impregnation method. Both the APC-2 laminates and the AS4/PEEK prepregs used the untreated, size-free Hercules AS4 as reinforcement.

Two types of Ply-Simulated-Laminates (PSL) [22] in the form of $[0_{16}]$ and $[(0/90)_2]_8$ laminates, referred to as unidirectional composites (UDC) and cross-ply laminates (XDL) in the following text, were molded from the prepreg with a matched mold in a programmable hot-press, one with constitutive ply number, $n_{\mathrm{CL}}$, of four and the other with $n_{\mathrm{CL}} = 2$. A thermosetting polyimide film 50 μm thick was used as the separation film. The cooling rate was kept constant at − 20°C/min for all laminate preparation.

Carbon fibers in the prepregs and the laminates were separated from the matrix polymer with either sulfuric acid and/or chlorophenol. When sulfuric acid was used, a $25 \times 25\ \mathrm{mm}^2$ composite specimen was kept in the acid for a fortnight at room temperature. The obtained fiber bundles (AS4–S) were then washed with enough 0.1 N sodium carbonate solution and then with sufficient deionized water. Extraction with chlorophenol was performed in a Soxhlet apparatus for over 60 h. The isolated fiber bundles (AS4–Cl) were further extracted with acetone for 12 h to remove any residual solvent. All these fibers were then vacuum-dried at room temperature and will be referred to as ‘extracted fibers’ in this paper. Gravimetric measurement revealed that the fiber content in the composites studied here is no less than 0.6675 by weight.

To obtain PEEK coated carbon fibers, bundles of AS4 fiber, hand-wound on a polytetrafluoroethylene (PTFE) fixture, were immersed in a chlorophenol solution of PEEK and de-gassed in a vacuum oven at 150°C for 15 min. Excess solution was then squeezed off with another PTFE blade. The AS4 fiber soaked in the PEEK solution in this way was then vacuum-dried at 150°C to remove the solvent. Supposing the fiber bundle has a random-stacked cross-section and the amount of residual solvent is negligible, then the average thickness of the resin layer on the fiber surface can be estimated by: $d_{\mathrm{f}}[(1 + w_{\mathrm{f}}/2)^{1/2} - 1]/2$, in which $d_{\mathrm{f}}$ is the fiber diameter and $w_{\mathrm{f}}$ the weight concentration of polymer solution. Melting of the coated fiber was performed using a nitrogen-purged stove. The stove allowed the heating and cooling rates to be 20°C/min. The highest temperature during the treatment was 400°C.

X-ray photoelectron spectra (XPS) were collected with a Vacuum Generators’ Escalb MK II X-ray photoelectron spectrometer. Typical resolution was 0.8 eV at 240 W (Mg K$\alpha$, 12 kV). For purposes of correction of specimen charging, the C1s bands were calibrated by assuming the binding energy of the benzene peak to be 284.6 eV. Fourier transform Raman (FT-Raman) spectra were obtained with back-scattering geometry in a Bruker RS100 FT-Raman spectrometer (laser source, $\mathrm{Nd}^{3+}$:YAG at 1064 nm, power, 40–60 mW, sampling step, 4 $\mathrm{cm}^{-1}$). Each spectrum was the cumulative result of 500 scans unless otherwise notified. The major problem in collecting composite spectra arose from a thermal band, centered around 3160 $\mathrm{cm}^{-1}$ with a Lorentzian profile. Absorption by carbon fiber and the poor thermal conductivity of the polymer were believed to be the main causes for this noise. The problem was circumvented by either sampling over a narrow wavenumber range

Table 1
Surface composition of carbon fibers[a]

| Fiber | C/C | N/C | O/C | Cl/C | Na/C | S/C |
|---|---|---|---|---|---|---|
| AS4 | 100 | 4.188 | 21.07 | — | 0.381 | — |
| AS4–Cl | 100 | — | 20.12 | 1.091 | — | — |
| AS4–S | 100 | 1.731 | 20.72 | 0.247 | 0.742 | 0.742 |

[a] Atomic ratio based on carbon.

(for fibers) or by subtracting a best-fit Lorentzian component centered around 3200 $\mathrm{cm}^{-1}$ with about 600 $\mathrm{cm}^{-1}$ width (for composites). When Raman bands have to be subtracted from an as-measured composite spectrum, the Lorentzian thermal band was subtracted from the latter at first, and then it was normalized over the wavenumber range between 100 and 3500 $\mathrm{cm}^{-1}$ according to the strength of the 1145 $\mathrm{cm}^{-1}$ PEEK skeleton vibration band [23]. A resin spectrum, which had also been normalized according to the PEEK skeleton band, was further subtracted from the obtained spectrum. Whenever spectra deconvolution had to be performed, Lorentzian functions were adopted.

## 3. Results and discussion

### 3.1. Structure of the extracted fibers

The results of the XPS study are presented in Fig. 1(a)–(c), illustrating O1s, N1s and C1s spectra of the AS4 fibers as-received and of the fibers isolated from APC-2 composites, respectively. According to the calculated surface composition of the fibers (Table 1), it can be seen that contents of chloride, sodium and sulfur in the extracted fibers are much lower than the oxygen fraction, suggesting negligible effects of the residual solvents. The nitrogen content of the original AS4 fiber determined in this work agrees well with the literature data [24]. In comparison to this, the lower nitrogen content of the surfaces of the extracted fibers is indicative of fiber surface modifications resulting from either the extraction or melt processing of the composites. Nitrogen is usually rich on the surface layer, dozens of nanons thick in the PAN-based carbon fiber [25]. The mean free path of the C1s and N1s photoelectrons from ordinary polymers is of the order of 3 nm [26]. With the emission angle of the photoelectron being 90° in the present XPS experiments, the sampling depths of the photoelectron here should be about 10 nm. This means that removal of the nitrogen-containing layer from the fiber is unimaginable. As a result, the decrease in nitrogen content of the extracted fibers strongly suggests the existence of an anchored layer of the aromatic polymer that muffled the fiber surface during melt processing with a thickness that is identical to the sampling depth of the photoelectron, i.e. 10 nm [26].

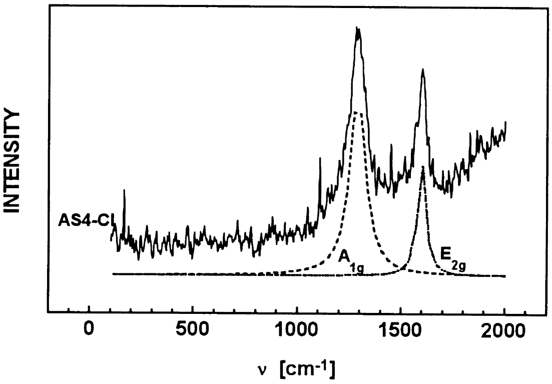

Fig. 2. FT-Raman spectrum of the carbon fibers extracted from its PEEK powder prepregs by chlorophenol.

Although specimen charging and mathematical uncertainty in C1s deconvolution prevent the authors from analyzing the exact composition of the fiber surface, C1s and O1s profiles would further confirm the analysis. From Fig. 1(a), it can be found that oxygen 1s spectra of the acid-extracted fibers lost the two-component feature that characterized AS4 fiber surface. Oxidization by the concentrated sulfuric acid near the fiber surface can be expected during extraction. In contrast, O1s profile of the fibers isolated by chlorophenol shows no more than an increase in relative content of oxygen atoms in a more reductive chemical environment.

Similarly, C1s spectra also show the difference between the extracted fibers and the as-received one. From Fig. 1(c), it can be seen that there is no distinctive $\pi-\pi^*$ peak on the spectra of these three sorts of fibers. Leveling-off at binding energy higher than 291 eV can be found instead, indicating that the surface of the fibers is highly aromatic and possesses a complex structure. The smoothly decreasing shoulder between the peak at 284.6 eV and the carboxyl 289 eV, on the other hand, suggests the diversity in the chemical environment of the C–O and C=O bonds. Therefore, higher shoulder intensity of C1s spectra of the extracted fibers (Fig. 1(c)) manifests that more carbon atoms should take the form of diphenyl ether and ketone in the extracted fibers. Considering the fact that oxygen on the AS4 fiber surface is predominantly presented in the form of phenol and carboxyl [27], the above results show clearly that there is an anchored layer of etheretherketone segments on the surface of the extracted fibers. The strong interaction between fiber surface and polymer matrix can be formed only through the processing.

Fig. 2 illustrates the FT-Raman spectrum of the carbon fiber isolated from AS4/PEEK prepregs with chlorophenol extraction. It can be seen that the spectrum is characterized by the two broad bands centered around 1600 and 1290 $\mathrm{cm}^{-1}$, respectively. Since the AS4 fiber is a PAN-based carbon fiber consisting of highly orientated graphite crystallites [24], the two bands should be attributed to the micro-crystalline structure of graphite. The results of lattice dynamics [28] show that the zone-center optical modes of graphite can be expressed as

$$\Gamma = A_{2u} + 2B_{2g} + E_{1u} + 2E_{2g} \quad (1)$$

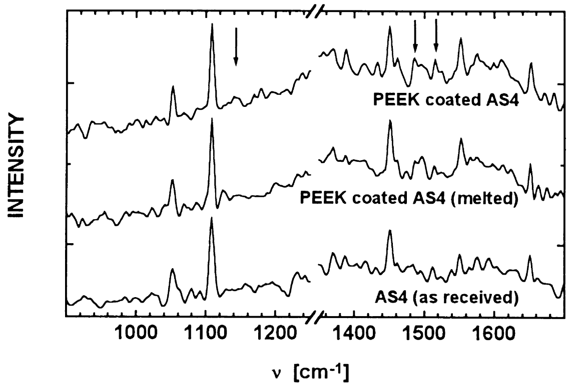

Fig. 3. Raman bands of the coated fibers in comparison to those of the uncoated version. (Each spectrum was obtained with 2000 scans and had been normalized to intensity of its lower wavenumber fluorescence peak, at around 281 cm$^{-1}$, before subtraction. Estimated coating thickness: 4.7 nm.)

Except for the optical-inactive $B_{2g}$ and the infrared-active $A_{2u}$ and $E_{1u}$ modes, the Raman-active mode, $E_{2g}$, was found at 42 and 1581 cm$^{-1}$. For micro-crystalline graphite, Tuinistra and Koenig [29] discovered another mode, $A_{1g}$, at 1355 cm$^{-1}$, which was believed to be related to the crystal boundary. The scattering intensity ratio, $I(E_{2g})/I(A_{1g})$, was found to be related to the micro-crystalline ordering and bulk modulus of the graphite fiber [29] and used in characterizing graphitization of carbon fibers [30]. In addition, the Raman shift of $E_{2g}$ was applied to a micromechanics investigation of carbon fiber reinforced composites [31]. Therefore, the band at 1600 cm$^{-1}$ in Fig. 2 no doubt belongs to the $E_{2g}$ mode of the carbon fiber.

Although the lattice dynamics of the $A_{1g}$ mode remain a subject for debate [28], its dispersive nature dictates that the Raman band should depend on the exciting frequency. In fact, Vidano and co-workers [32] have found a decrease in the Raman shift by 35 cm$^{-1}$ per 5000 cm$^{-1}$ of exciting wavenumber when the exciting wavelength increased. A similar property of $A_g$ mode was also observed in polyacetylene [33]. In consideration of the fact that the laser source of the current work emitted radiation with a wavelength of 1.064 μm, which was 11 093 cm$^{-1}$ lower in wavenumber than that used by Tuinistra and Koenig [29], the $A_{1g}$ mode should appear at 1277 cm$^{-1}$. Fig. 2 shows that the experimental result is in good agreement with the prediction. That is, the 1290 cm$^{-1}$ band can be confirmed as the dispersive branch of $A_{1g}$, indicating that the carbon fiber, compounded with polyetheretherketone, still possesses a micro-crystalline graphite structure of the turbostratic carbon.

On the other hand, the observed Raman shifts of the extracted fibers are all higher than the theoretical values, which implies an oxidative chemical environment at the edge of the graphite crystallites. Because the two Raman modes are related to the lattice of the graphite micro-crystals in nature, violet shifts of this kind demonstrate that the oxygen-containing functional groups of the matrix resin must have formed certain delocalized electron structures coupled with graphite crystallites. In comparison with the XPS results, it can be concluded that the ether and ketone groups of PEEK in the interfacial region tended to be in conjugation with the graphite layers of carbon fiber. In other words, electron interaction between the organic component and the fiber may be an additional aspect of the interfacial structure in the composite.

Table 2
Tentative assignment of the fiber surface Raman bands

| Assignment | AS4 | AS4 with PEEK coating | AS4 with PEEK coating, melted | Usual activity[a] | |
|---|---|---|---|---|---|
| | | | | IR | RS |
| C=O stretch | 1651.2 | 1653.1 | 1651.2 | s | s |
| 6-member ring stretch | 1591.4 | 1608.8 | — | s | s |
| (quadrant) | 1574.1 | 1576.0 | 1576.0 | | |
| Carbon fiber skeleton (5-member ring) | 1550.9 | 1552.8 | 1552.8 | d | d |
| 6-member ring stretch[b] (semi-circle) | 1512.3 | 1516.2 | — | s | w or n |
| | 1485.4 | 1487.3 | 1496.9 | | |
| Carbon fiber skeleton (*trans* CH rock) | 1450.6 | 1450.6 | 1450.6 | | m to s |
| PEEK skeleton[b] (*cis* CH rock) | — | 1414.0 | — | s | n |
| ring C–O vibration | 1369.6 | 1388.9 | 1369.6 | s to w | n |
| | 1321.4 | 1307.9 | 1302.2 | | |
| C–O–C skeleton vibration | 1157.5 | 1142.1 | 1124.7 | m | s to m |
| CF skeleton (conj. C=C) | 1109.3 | 1109.3 | 1109.3 | | s to m |
| =CH wagging | 926.1 | 916.4 | 955.0 | s | w |
| ring bending | 839.3 | 833.5 | 835.4 | | |

[a] s: strong; d: both active; w: weak; n: non-active; m: active with moderate intensity.

[b] Aromatic ether and ketone band normally only IR-active in PEEK.

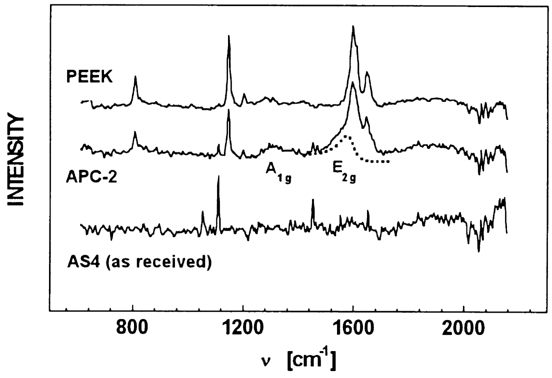

Fig. 4. Recorrected Raman spectra of PEEK, APC-2 and AS4 fibers. (For APC-2 and AS4, a thermal band at 3160 $\mathrm{cm}^{-1}$ and two fluorescent bands with a width of more than 600 $\mathrm{cm}^{-1}$ were subtracted. No thermal band was observed in the spectrum of PEEK, from which only the fluorescence components were removed.)

### 3.2. Structure of the thin layer of PEEK coated on a carbon fiber

The AS4 carbon fiber coated with a thin layer of PEEK was studied to simulate the formation of the above interfacial structure. Fig. 3 illustrates the FT-Raman spectra of the AS4 fiber, the fiber coated with PEEK, and the coated fiber that had experienced heat treatment at 400°C, respectively. In order to analyze the surface functional groups, the spectra were collected with 2000 scans. It was found that with a longer sampling time, the thermal band (centered around 3200 $\mathrm{cm}^{-1}$) was much stronger and resulted in large uncertainty in analyzing Raman bands with moderate width of dozens of reciprocal centimeters. Several narrow bands that related to functional groups of the fibers (Table 2), however, are quite distinctive in the spectra. Taking notice of the fact that the relative intensities of these bands are close to what was found with shorter sampling time (Fig. 2), the four strongest bands (1063, 1109, 1451 and 1651 $\mathrm{cm}^{-1}$) can be assigned to the conjugated $sp^2$ carbon in the turbostratic packing of graphite layers of carbon fibers and the oxygen-containing groups on the fiber surface. Intensities and Raman shifts of these bands are almost the same in these three spectra (Fig. 3), supporting the above argument that the bulk structure of the carbon fiber remained unchanged through wetting with PEEK.

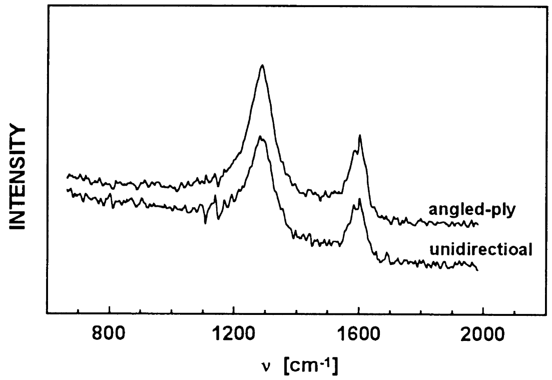

Fig. 5. Raman spectra of typical AS4/PEEK PSL plates ($n_{\mathrm{CL}} = 4$) after removal of the matrix resin bands.

Unlike the above four stronger bands, Raman scattering at around 1500 $\mathrm{cm}^{-1}$ is quite different in the three spectra. In the spectrum of the un-coated AS4 fiber, there is no discernible feature within this range of wavenumber. In contrast, a doublet at 1512/1485 $\mathrm{cm}^{-1}$ can be found in the spectrum of the coated fiber, which further turned to the 1497 $\mathrm{cm}^{-1}$ band in that of the melted coating version. Since XPS study of the coated fiber shows no more than coverage of the fiber surface by the polymer, the bands should be attributed to polyetheretherketone. The quadrant stretching mode of the rings, which is observable usually only in infrared-active neat PEEK [34,35], also became Raman-active when the polymer was adjacent to the carbon fiber surface. Due to the fact that a change in a vibrational mode from IR-active to Raman-active reflects an increase in polarizability [36], the above result suggests that the electron structure of PEEK near the fiber surface must be more de-localized than usual. Obviously, PEEK in this special conformation can form an electron interaction with the graphite layers of the carbon fiber.

### 3.3. Interfacial Raman spectra of AS4/PEEK composites

Fig. 4 shows the recorrected Raman spectrum of an as-received APC-2 laminate in comparison with the spectra of the AS4 fiber and PEEK. Because only Lorentzian shape bands with a width much greater than those of $A_{1g}$ and $E_{2g}$ modes had been subtracted during spectra recorrection processes, each spectrum in Fig. 4 can be considered to be the result of neat Raman scattering from the correspondent materials. It can be seen that the laminate spectrum predominantly consists of Raman bands of AS4 fiber and PEEK. Coinciding with the infrared spectroscopy [37], the strong PEEK scattering indicates the presence of a surplus resin layer on the laminate surface. Besides, two weak components can also be found from the laminate spectrum, one near 1300 $\mathrm{cm}^{-1}$ with a Lorentzian band shape, another near 1585 $\mathrm{cm}^{-1}$ with a profile that can be most properly described with the Breit–Wigner–Fano (BWF) equation: [38,39]

$$I(\omega) = I_0[1 + (\omega - \omega_0)/(q\Gamma)]^2[1 + (\omega - \omega_0)^2/\Gamma^2]^{-1} \qquad (2)$$

where $I_0$ is a normalization factor, $\omega_0$ the renormalized resonant frequency corresponding to $I_0$, $\Gamma$ a measure of the linewidth and $q^{-1}$ the BWF coupling coefficient [40]. Similar features can also be found in the difference spectra of the home-made AS4/PEEK laminates with a thinner surface resin layer (Fig. 5). The BWF lineshape in Raman scattering arises from the interaction between discrete Raman-active phonon modes and a continuum of Raman excitations [39,40]. So far there is no evidence of increased disordering in the carbon fiber, the resonance must have originated from

Table 3
BWF factors and Raman shifts of $E_{2g}$ and $A_{1g}$

| | $E_{2g}$ and ring band | | | Dispersion band | | |
|---|---|---|---|---|---|---|
| | $\omega_0$, cm$^{-1}$ | $\Gamma$ | $-q$ | $\omega_0$, cm$^{-1}$ | $\Gamma$ | $-q$ |
| AS4–Cl | 1604.01 | 26.16 | 10.77 | 1288.66 | 43.38 | 36.06 |
| XDL($n_{CL} = 4$) | 1613.39 | 37.36 | 3.10 | 1294.49 | 39.43 | 8.78 |
| UDC($n_{CL} = 4$) | 1610.44 | 37.82 | 3.39 | 1314.56 | 34.62 | 2.25 |

an interaction between fiber and polymer at the boundary of the graphite crystallites near the fiber surface.

### 3.4. Intercalation analogy

Since the first-order bands of the interfacial spectra have been proved to possess BWF lineshape, an analogy to intercalation can be drawn to analyze the interfacial structure of the composites. Curve fitting of the spectra in Fig. 5 according to Eq. (2) yields $q$ values as listed in Table 3. It is interesting to note that the values of $q$ are close to that of the stage-1 alkali metal compounds, such as $C_8Cs$ [40]. If the analogy works, the broad band at around 1600 cm$^{-1}$ should consist of two Lorentzian components, $E_{2g0}$ of graphite interior layers and $E_{2g}$ of boundary layers, which are in turn near 1582 cm$^{-1}$ and a higher wavenumber, respectively [40,41]. Spectra deconvolution shows that it is true for a typical difference spectrum (Fig. 6). The Lorentzian center of the latter component varies from 1604 to 1613 cm$^{-1}$ for different AS4/PEEK composites. Compared to the dependence of Raman frequencies of the intercalated compounds on reciprocal stage number, $1/n$ [40], the value indicates a stage number, $n$, of about 2 to 3 if the intercalant is of donor type, or of about 3 had it been of acceptor structure. The result suggests that there should be one layer of ether ether ketone segments (EEK) for two to three layers of graphite layer on the fiber surface. Such a presumed super-lattice is in agreement with the $10^0$ nm periodicity found on the surface of PAN-based carbon fibers with an atomic force microscope by Krekel and co-workers [42], which further proves the validity of the above analogy, implying that an intercalation-type interaction must have formed between the fiber and the polymer. In conjunction with the previous results from spectra studies of the extracted fibers, this model may account for the interfacial structure in the composites. In other words, a strong interface should originate, at least partly, from the electronic interaction between PEEK segments in co-planar conformation and graphite crystallites in the carbon fiber.

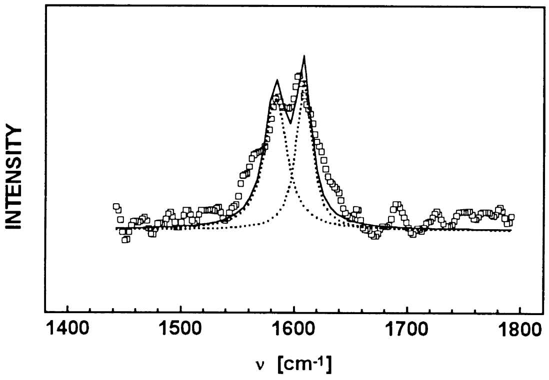

Fig. 6. Two-order Lorentzian best fit to the difference spectrum of the surface ply in an angled PSL plate (XDL, $n_{CL} = 4$).

## 4. Conclusion

It has been proved that PEEK chains tended to anchor on a carbon fiber in the composites. Melting of polymer played an important role in the absorbing process. No clear evidence was found for any chemical bonds between the two components. In contrast, conjugation between graphite crystallites and aromatic polymer were evident, indicating that it is possible for the polymer to form strong short-range interaction with fiber reinforcement through mechanisms other than chain-end bonding. Reaction mechanism and kinetics of the strong interaction remain to be studied further.

With the successful data treatment, Raman scattering of carbon fiber in practical composites was separated from macroscopic FT-Raman spectra of the composites. Lineshape analyses of the difference spectra allowed us to probe into the nature of the interfacial interaction. Through the analogy of the interfacial interaction to graphite intercalation compounds, it has been demonstrated that ether ether ketone segments tended to form structures similar to stage-2–stage-3 graphite intercalation. The analogy further proved that the electron interaction at the boundary of graphite crystallites of a carbon fiber contributed much to the composite interfacial structure.

It should be mentioned that diffusion of PEEK chains was not considered in the present analyses. It is believed that studies of model systems, as employed in researches on thermosetting composites [8–12], would help to assess whether the interaction is only near the fiber surface or involves the bulk structure of fiber reinforcement. When the chemical structure of the anchored polymer in such a model system is fully characterized, it would be able to say whether physical bonding through non-end group segments may also be one of the general features of carbon fiber composites with the linear aromatic polymers as matrix materials.

## Acknowledgements

The authors express their thanks to Prof. Gi Xue, Dr Yun Lu, Dr Shi Jin, Dr Fengting Li, Dr Zhongren Yue and Mr Rong Zeng for the help received. The support of the National Natural Science Foundation of China (Grant No. 59725307), the Trans-Century Training Programme Foundation for the Talents of the State Education Commission of

China are gratefully acknowledged. Dr T. Q. Li is grateful to the support of the Laboratory of Polymeric Composite and Functional Materials, The State Educational Commission of China (Grant No.19703).

## References

[1] Erickson PW, Plueddemann EP. In: Plueddemann EP, editor. Interfaces in polymer matrix composites. New York: Academic Press, 1974:2.
[2] Drzal LT, Rich RJ, Lloyd PF. J Adhes 1983;16:1.
[3] Asloun ElM, Nardin M, Schultz J. J Mater Sci 1989;24:1835.
[4] Hughes JDH. Compos Sci Technol 1991;41:13.
[5] Kim J-K, Mai Y-W. Compos Sci Technol 1991;41:333.
[6] Young PR, Chang AC. SAMPE Q 1986;17(4):32.
[7] Li T, Zhang M, Zeng H. Gaofenzi Cailiao Kexue Yu Gongcheng (Polymeric Materials Science and Engineering) 1997;13(5):15.
[8] Koenig JL, Shih PTK. J Colloid Interf Sci 1971;36:247.
[9] Ishida H, Koenig JL. J Colloid Interf Sci 1978;64:555.
[10] Garton AJ. Polym Sci, Polym Chem Ed 1984;22:1495.
[11] Hoh K-P, Ishida H, Koenig JL. Polym Compos 1990;11:192.
[12] Sellitti C, Koenig JL, Ishida H. Mater Sci Eng 1990;A126:235.
[13] Papenicolaou GC, Paipetis SA, Teocaris PS. Colloid Polym Sci 1978;256(7):625.
[14] Drzal LT. SAMPE J 1983;19(Sep/Oct):7.
[15] Theocris PS, Spathis G, Kefalas B. Colloid Polym Sci 1982;260:837.
[16] Brady RL, Porter RS, D'Onovan JA. J Mater Sci 1989;24:4138.
[17] Stone PR, Nairn JA. Polym Compos 1994;15:197.
[18] Nardin M, Asloun EM, Schultz J. Surf Interf Analysis 1991;17:485.
[19] Pisanova EV, Zhandarov SF, Dovgyalo VA. Polym Compos 1994;15:147.
[20] Vu-khanh T, Denault J. J Reinf Plast Compos 1993;12:916.
[21] Zhang M, Xu J, Zhang Z, Zeng H, Xiong X. Polymer 1996;37:5151.
[22] Manson J-AE, Seferis JCJ. Compos Mater 1992;26:405.
[23] Louden JD. Polym Commun 1986;27:82.
[24] Drzal LT, Rich MJ, Koenig MF, Lloyd PF. J Adhes 1983;16:133.
[25] Yue ZR. PhD Thesis, Zhongshan University, Guangzhou, China, 1995.
[26] Wang J, Wu W, Feng D. Introduction to electron spectroscopy (XPS/XAES/UPS). Beijing: Defense Industry Press, 1992:246.
[27] Sellitti C, Koenig JL, Ishida H. In: Ishida H, editor. Interfaces in polymer, ceramic, and metal matrix composites. New York: Elsevier, 1988:163.
[28] Nemanich RJ, Solin SA. Phys Rev B 1979;20(2):392.
[29] Tuinistra F, Koenig JL. J Chem Phys 1970;53:1126.
[30] Cottinet D, Couderc P, Saint Roman JL, Dhamelincourt P. Carbon 1988;26:339.
[31] Gu X, Young RJ, Day RJ. J Mater Sci 1995;3:1409.
[32] Vidano RP, Fischbach DB, Willis LJ, Loehr TM. Solid State Comm 1981;39:341.
[33] Horovitz B. Synthetic Metals 1984;9:215.
[34] Cole KC, Casella IG. Polymer 1993;34:740.
[35] Li T. PhD Thesis, Zhongshan University, Guangzhou, China, 1997.
[36] Xue G. Spectroscopy methods in studies of polymer structure. Beijing: Higher Education Press, 1995.
[37] Chalmers JM, Mackenzie MW. In: Mackenzie MW, editor. Advances in applied Fourier transform infrared spectroscopy. Chichester: John Wiley and Sons, 1992:138.
[38] Scott JF. Rev Mod Phys 1974;46:83.
[39] Klein MV. In: Cardona M, editor. Light scattering in solids, Chapter 4. Berlin: Springer, 1975.
[40] Dressehauls MS, Dressehauls G. In: Cardona M, Guntherodt M, Guntherodt G, editors. Light scattering in solids III, recent results. Berlin: Springer, 1982:1.
[41] Eklund PC, Subbuswamy KR. Phys Rev 1979;B20:5157.
[42] Krekel G, Hunttinger KJ, Hoffman WP, Silver DS. J Mater Sci 1994;29:2968.